DOI: 10.1017/S1431927605508523

Microsc Microanal 11(Suppl 2), 2005

Imaging of Non-conductors by Ultra-high Resolution Immersion Lens SEM

M. Toth,* B.L. Thiel** and W.R. Knowles*

* FEI Company, 1 Corporation Way #2, Peabody, MA, USA 01960.
** College of Nanoscale Science and Engineering, University at Albany – SUNY, 255 Fuller Rd, Albany, NY, USA 12203

A new SEM technique is presented for ultra-high resolution imaging of samples that charge too severely for imaging by low voltage microscopy. The new approach is facilitated by a recently developed low vacuum secondary electron detector that can operate in the presence of the magnetic field of an immersion objective lens [1]. Imaging examples are shown in Fig. 1: (a) a pit in SiO_2, (b) a Cr on quartz photomask, and (c) a contact hole in SiN.

In high vacuum SEM, insulators and electrically floating conductors can be imaged using low beam energies (typically, ~ 1 keV). In theory, the beam energy is fine tuned so as to make the total yield (i.e., the sum of the secondary and backscattered electron coefficients δ and η) equal to unity, so that the net charge buildup rate inside the sample is equal to zero [2,3]. However, in reality, this critical beam energy varies within any contrast-containing image (since all image contrast corresponds to variations in δ and/or η). Consequently, samples charge dynamically during imaging and the surface potential fluctuates during image acquisition. Such fluctuations serve to defocus the beam, distort the scan patter and modulate the electron imaging signal.

Fig. 2a shows a high vacuum secondary electron image of a via that had been cut into SiO_2 using a focused ion beam (FIB). The image was obtained using an accelerating voltage of 752 V, selected so as to minimize charging artifacts. The images contain regions that are in focus (indicated by arrows), but the via is blurred. This is seen more clearly in the elevated magnification image shown in Fig. 2b. At this increased magnification, it was not possible to improve the focus due to differential charging of the via sidewalls with respect to the surface normal to the beam. Low vacuum images of the same region, obtained using the Helix detector [1] of a FEI Nova NanoSEM, are shown in Fig. 2d-f. In these images, the focus is maintained across the entire field of view (see, for example, the features indicated by arrows on Fig. 2e). In addition, the images contain contrast (indicated by red arrows in (d) and (f)) that is absent in the high vacuum images shown in Fig. 2a-c. Such contrast is only visible in images of uncoated insulators, acquired using high beam energies. It is therefore not attainable by high vacuum SEM because chronic charging artifacts overwhelm all useful contrast. This is illustrated by the image shown in Fig. 2c, obtained in high vacuum using an accelerating voltage of 1.3 kV.

The effectiveness of low vacuum charge control is limited by the ability of the system to respond to dynamic changes in charging behavior during image acquisition (i.e., charge control "self-regulation") [4, 5]. We will discuss how imaging artifacts produced by self-regulation mechanisms can be minimized through the use of detector structures designed to auto-regulate the flux of ionized gas molecules incident onto the sample surface.

References
[1] B.L.Thiel, et al., *Microsc. Microanal* 10 (Suppl. 2) (2004) 1058.
[2] D.C. Joy & C.S. Joy, *Micron* 27 (1996) 247.
[3] J. Cazaux, *J. Appl. Phys.* 85 (1999) 1137.
[4] J.P. Craven *et al.*, *J. Microsc.* 205 (2002) 96.
[5] M. Toth *et al.*, *J. Appl. Phys.* 91 (2002) 4492.
[6] W.R. Knowles et al. (2005) elsewhere in these proceedings.

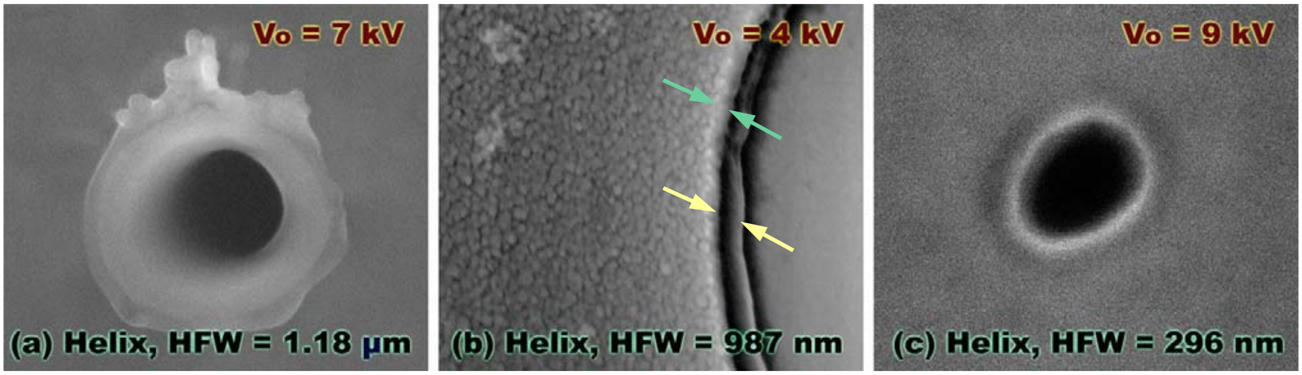

FIG. 1. Low vacuum, Helix detector images of a pit in SiO_2 (a), a Cr on quartz photomask (b), and a contact hole in SiN (c). In (b), green and yellow arrows point to the Cr absorber and an underlying quartz step, respectively (the region to the right of the step is the quartz substrate). [V_o = accelerating voltage, HFW = horizontal field width.]

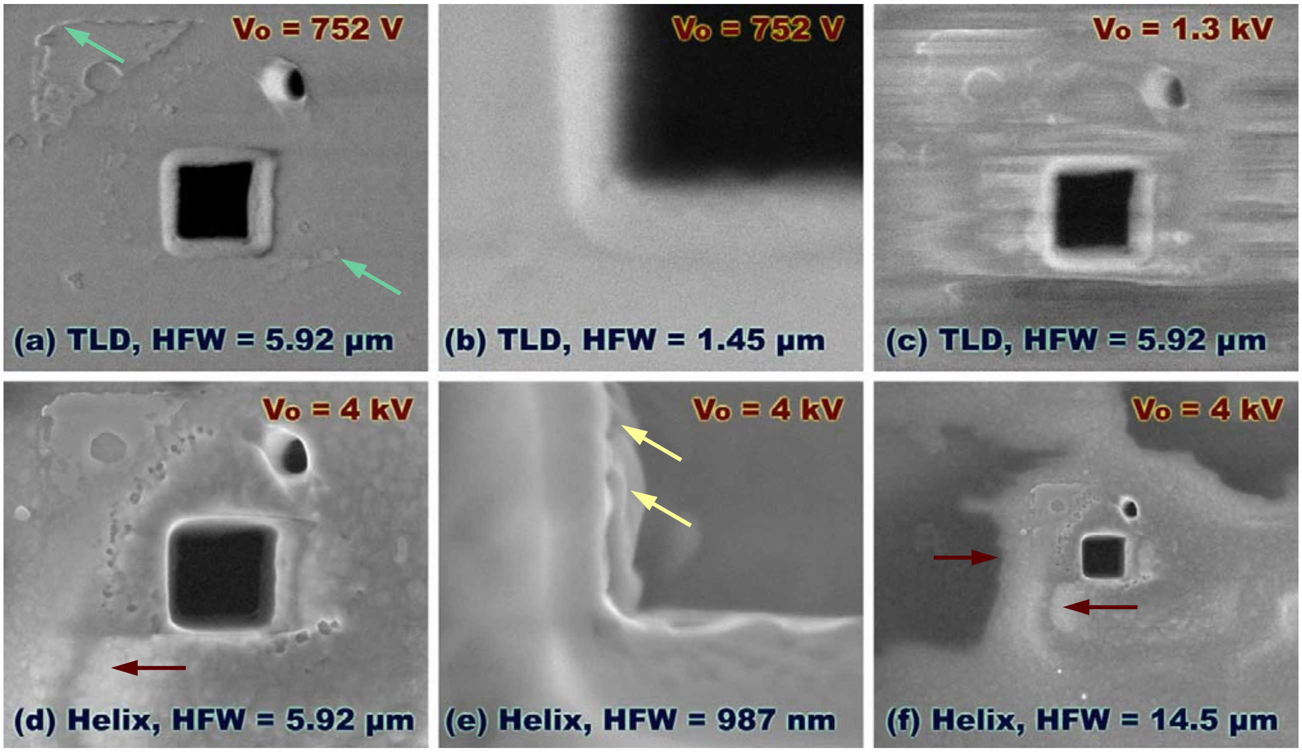

FIG. 2. Secondary electron images of a via in SiO_2, obtained in high vacuum using a through the lens detector (a-c), and in low vacuum using a Helix detector (d-f). The features indicated by arrows are discussed in the main text.